Transverse-momentum distribution of dileptons in different scenarios for the QCD phase transition

J. Cleymans,* J. Fingberg, and K. Redlich†
Fakultät für Physik, Universität Bielefeld, Federal Republic of Germany
(Received 7 July 1986; revised manuscript received 2 October 1986)

The transverse-momentum distribution of lepton pairs produced in ultrarelativistic nuclear collisions is analyzed in different scenarios for the phase transition from quarks and gluons to hadrons. A first-order phase transition at equilibrium is characterized by an intermediate phase where quarks, gluons, and hadrons coexist for an appreciable amount of proper time. The subsequent transition from one phase to the other is therefore very smooth. This is reflected in the dilepton production rate by a smooth change from the small- to the large-dilepton-invariant-mass region. A detonation is characterized by substantial supercooling of the quark-gluon-plasma phase with a subsequent superheating of the hadronic phase. The superheating is so intense that the dilepton rate arises almost completely from the hadronic phase, leaving almost no trace from the quark-gluon phase. A second-order phase transition is characterized by an instantaneous transition from one phase to the other. This reflects itself in a clean separation in the invariant mass in the dilepton production rate. It is suggested that experimental measurement of the average transverse momentum as a function of the invariant mass might help considerably in determining the dilepton production mechanism and through it reveal part of the evolution of the quark-gluon-plasma phase to the hadronic phase.

I. INTRODUCTION

The aim of this work is to examine the dilepton yield in high-energy nuclear collisions in different scenarios for the phase transition from quarks and gluons to hadrons. The precise thermodynamic mechanism for this transition is not known at present and, lacking further information on its space-time evolution, several paths appear to be equally plausible presently. Different possibilities will be investigated successively. A first-order phase transition is characterized by latent heat, by a possible coexistence phase between hadrons and quarks and gluons, and by a finite correlation length. The latent heat could cause the transition to proceed via supercooling of the quark-gluon-plasma phase to a subsequent violent superheating of the hadronic phase.[1] A first-order phase transition could also proceed via a Maxwell construction where the system spends an appreciable amount of time going through a mixed phase before turning to a purely hadronic system. A second-order phase transition, on the other hand, is not accompanied by the production of latent heat nor is there a coexistence phase but the correlation length becomes infinite at the critical temperature and the system changes instantaneously from one phase to the other.

In this respect, lepton pairs are a highly valuable source of information on the evolution of the system since they are emitted continuously and do not suffer rescattering as they have no strong interactions.[2] The bulk of the hadronic material, in contrast, provides information about the time when the system is at freeze-out temperature. Clearly the yield of dileptons will be sensitive to the scenario which is being followed by the system and it is the purpose of the present paper to point these differences out wherever they arise. To start our discussions we explain the equation of state used, respectively, for first- and second-order phase transitions. For the space-time dependence of the temperature we will use Bjorken's scaling solution for longitudinal hydrodynamic expansion.[3] This solution has been discussed repeatedly in the recent literature and we limit ourselves to emphasizing one of its physical assumptions.[4] In the central region of rapidity the system is assumed to have a plateau structure. This is known to be approximately correct for the final state of high-energy $p\bar{p}$ collisions. It implies that to a reasonably good approximation all thermodynamic quantities depend on the proper time τ but not on the rapidity variable y. For a nondissipative system, this solution leads to conservation of the entropy current and, in particular, for the case of one-dimensional expansion one finds

$$s\tau = \text{const} , \tag{1}$$

where s is the local entropy density.

The dilepton production rate and especially the transverse momentum p_T show interesting features when considered as a function of the invariant mass M. The invariant mass is relevant because heavy lepton pairs can only be produced when the system is at a high temperature, i.e., in the quark-gluon phase, while low-mass dileptons are produced predominantly in the hadronic phase where the temperature is low. The separation between the two phases is not always very clean. For example, for a first-order phase transition at equilibrium there exists a long-lived intermediate region where both phases coexist at the same temperature. This reflects itself in a broad overlap region; dileptons with an invariant mass between 1 and 2.5 GeV are produced either in the quark-gluon phase or in the hadronic phase with no clean separation possible. Above 2.5 GeV the quark-gluon-phase contributions dominate and below 1 GeV the hadronic-phase contributions dominate. For a second-order phase transition the coexistence region is completely absent and the transition from one phase to the other is instantaneous. This reflects itself in a much narrower overlap region; already above 1.6 GeV the quark-gluon phase completely dominates.

The dependence of the dilepton production rate should be considered with the above results in mind. For invariant masses below 1 GeV the production mechanism is dominated by the hadronic phase and the transverse momentum will behave accordingly. Above 2.5 GeV for a first-order transition and above 1.6 GeV for a second-order one the production mechanism changes and the transverse momentum reflects the quark-antiquark-annihilation mechanism. This change in mechanism will be the main focus point of this work.

Our choice of parameters may seem somewhat peculiar to the reader (initial temperature = 284 MeV, critical temperature = 227 MeV, freeze-out temperature = 154 MeV). They were forced upon us by the availability of results from lattice QCD and by the value of the QCD lattice parameter $\Lambda_L = 1.5$ MeV as explained below. For ready comparison between different scenarios we used these parameters consistently for all our calculations.

The plan of this paper is as follows. In Sec. II we present, for completeness, the equations of state we use as well as the space-time evolution of the temperature for different scenarios. In Sec. III we present the formulas used for the dilepton production rates. In Sec. IV we discuss the results we obtain for different scenarios and investigate their dependence on the parameters chosen. In Sec. V a summary of our results is given.

II. EQUATION OF STATE AND TEMPERATURE EVOLUTION

A. First-order phase transition

The most widely considered model for a first-order phase transition is based on the bag-model equation of state. The energy density, pressure, and entropy density in the high-temperature, baryonless quark-gluon-plasma phase in this model are given by

$$p_q = \frac{37\pi^2}{90} T^4 - B \ , \tag{2a}$$

$$\epsilon_q = \frac{37\pi^2}{30} T^4 + B \ , \tag{2b}$$

$$s_q = \frac{4}{3}\frac{37\pi^2}{30} T^3 \ , \tag{2c}$$

for two massless up- and down-quark flavors. B is, as usual, the bag constant. For the hadron phase we consider a gas of pions with the following equation of state:

$$p_h = \frac{\pi^2}{30} T^4 \ , \tag{3a}$$

$$\epsilon_h = \frac{\pi^2}{10} T^4 \ , \tag{3b}$$

$$s_h = \frac{2\pi^2}{15} T^3 \ . \tag{3c}$$

Keeping the pion mass different from zero leads to deviations from the above equations which are at most 20% in the temperature range under consideration. We consider the following possible scenarios.

1. Equilibrium phase transition

If the transition from quarks and gluons to hadrons is fast, a Maxwell construction can be performed where the system remains continuously in thermal equilibrium. The one-dimensional hydrodynamic expansion leads to a decrease of the temperature as shown in Fig. 1. Several features are worth noticing. First of all, for reasonable values of the initial temperature, the system spends only a short fraction of its lifetime in the pure quark-gluon phase. Second, the mixed phase dominates completely. This is a consequence of the entropy law since the number of degrees of freedom in the quark-gluon phase is much larger than in the hadronic phase and therefore tends to inhibit the transition. If one takes into account the transverse expansion of the system, then its overall lifetime is reduced because the transverse rarefaction wave propagating inward provides for additional cooling of the system. The hadronic and intermediate phases will thus be shortened but the pure quark-gluon-plasma phase will not be affected substantially because of its short lifetime at the beginning of the system.

2. Supercooling with subsequent superheating

In case the transition from quarks and gluons to hadrons is inhibited by a slow hadronization rate, the system can become supercooled. Because of the latent heat there will be a subsequent violent transition to superheated hadronic matter. If there exists a sharp front separating

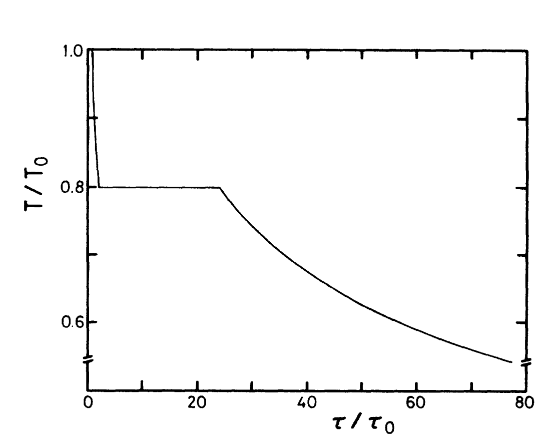

FIG. 1. Dependence of the temperature on proper time for a first-order phase transition (Maxwell construction). T_0 is taken to be 284 MeV, $\tau_0 = 1$ fm, $T_c = 227$ MeV, $T_{fo} = 154$ MeV.

both phases this is called a detonation. In this scenario, taking into account energy and momentum conservation, the dependence of temperature on proper time is shown in Fig. 2. One notes that the quark-gluon-plasma phase is being substantially supercooled and the subsequent transition to superheated hadronic matter leads to a big jump in the temperature. The history of the system is dominated by the long lifetime of the high-temperature hadronic phase. As a consequence the observed final state will show almost no trace of the initial quark-gluon-plasma phase.

3. *Deflagration*

Deflagrations were first proposed by van Hove[5] as a possible mechanism for the transition from quarks and gluons to hadrons. Again the transition rate is slow and the existence of a sharp front separating both phases is assumed. However, this time the transition starts slightly before it reaches the critical temperature and the produced hadrons are ejected from the system with large velocities but with very low temperatures, in fact even below most guesses for what the freeze-out temperature could be. This scenario has the peculiar property that the contamination from the hadronic phase is negligible. Of course, there are still contributions from that portion of the nuclei that were unaffected by the phase transition. This is, however, not the part we are focusing on.

B. Second-order phase transition

A second-order phase transition is more complicated to construct than a first order one. Because of the long-range correlations in the transition region one cannot derive an equation of state with each phase characterized by a noninteracting gas. Also by a more complicated model for the hadronic gas and interactions between constituents in the quark-gluon-plasma phase will still lead to a first-order phase transition by construction. Because of this we shall use the equation of state as derived from recent results from lattice QCD including fermions obtained in Ref. 6.

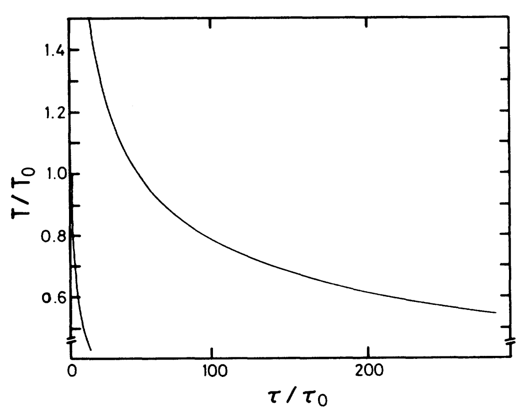

FIG. 2. As in Fig. 1, but for first-order phase transition with detonation.

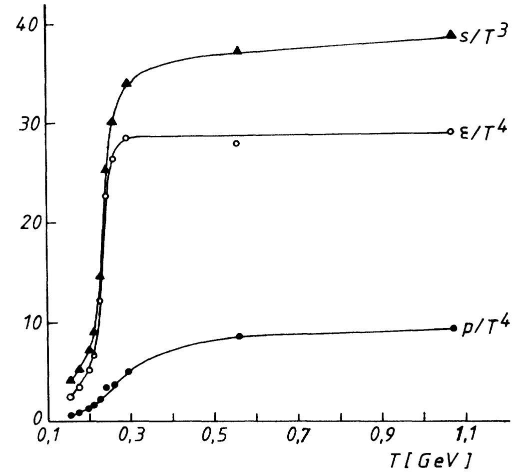

FIG. 3. Thermodynamic quantities as a function of temperature from lattice QCD (Ref. 6): P (pressure), ϵ (energy density), s (entropy density).

The results we need concern the behavior with temperature of the thermodynamic quantities pressure, energy density, and entropy density. They were obtained on an $8^3\times 3$ lattice with Wilson fermions in a fourth-order hopping parameter.[7] To relate the coupling constant g^2 to the temperature we used the renormalization-group equation obtained from the weak-coupling expansion of the β function to two-loop order for two flavors of fermions. The approximate value $\Lambda_L \simeq 1.5$ MeV was used for the lattice parameter. For completeness we present these results in Fig. 3. Combining this information with the scaling solution for longitudinal hydrodynamic expansion leads to the temperature decreasing with proper time as shown in Fig. 4. The transition is now instantaneous because the correlation length diverges at the critical temperature. Comparison of the temperature behavior with the equilibrium first-order transition shown in Fig. 1 indicates that the temperature is now consistently higher in the quark-gluon phase and consistently lower in the hadronic phase. This together with the change in dynamics leads to interesting differences in the dilepton production rate which we point out in the next section.

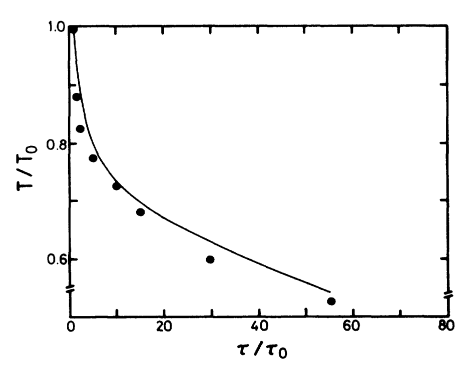

FIG. 4. As in Fig. 1 but for second-order phase transition.

III. PRODUCTION OF DILEPTONS

A. Rate in the quark-gluon-plasma phase

To calculate the production rate of dimuons in the quark-gluon plasma phase we use the expression

$$\frac{dN_Q}{d^4x\,d^4p}=\int\frac{d^3q}{(2\pi)^3}\frac{d^3\bar{q}}{(2\pi)^3}v_{q\bar{q}}\sigma(q\bar{q}\to\mu^+\mu^-)\times f_q f_{\bar{q}}\delta(p-q-\bar{q})\ , \tag{4}$$

where N_Q is the number of dimuons produced, d^4x is the infinitesimal space-time volume, p is the momentum of the dimuon, q ($\bar{q}$) is the momentum of the quark (antiquark), $v_{q\bar{q}}$ is the relative velocity, and $\sigma(q\bar{q}\to\mu^+\mu^-)$ is the electromagnetic cross section for the annihilation of a quark-antiquark pair into a dimuon:

$$v_{q\bar{q}}\sigma(q\bar{q}\to\mu^+\mu^-)=\sum_i e_i{}^2\frac{8\pi\alpha^2}{9M}\left[1+2\frac{m^2}{M^2}\right]\times\left[1-4\frac{m^2}{M^2}\right]^{1/2}. \tag{5}$$

e_i is the charge of the quark, α is the electromagnetic coupling, M the invariant mass of the dimuon, m the muon mass. The factors f_q and $f_{\bar{q}}$ are the momentum distribution functions of the quarks and antiquarks:

$$f_q=\frac{6}{e^{(u\cdot q-\mu)/T}+1}\ , \tag{6a}$$

$$f_{\bar{q}}=\frac{6}{e^{(u\cdot \bar{q}+\mu)/T}+1} \tag{6b}$$

with μ being the chemical potential and u^ν the local four-velocity of the plasma element. In the final analysis we will put μ equal to zero. If we restrict ourselves to the longitudinal expansion, u^ν can be parametrized as[8]

$$u_\nu=(\cosh\theta,0,0,\sinh\theta)\ , \tag{7}$$

where θ is the plasma rapidity given by

$$\theta=\text{arctanh}v \tag{8}$$

and v is the plasma velocity. In terms of θ and the rapidity Y of the lepton pair, one obtains

$$u\cdot q=M_T\cosh(\theta-Y) \tag{9}$$

with

$$M_T=(M^2+p_T{}^2)^{1/2} \tag{10}$$

being the transverse mass of the dimuon and with Y defined as

$$Y=\tfrac{1}{2}\ln\frac{E+p_Z}{E-p_Z} \tag{11}$$

its rapidity.

The integrals over quark and antiquark momenta can be performed analytically with the following result:

$$\frac{dN_Q}{d^4x\,d^4p}=\frac{\alpha^2}{4\pi^4}\left[1+\frac{2m^2}{M^2}\right]\left[1-\frac{4m^2}{M^2}\right]^{1/2}\times e^{-E/T}K_Q(p,T,\mu)\sum_i e_i{}^2\ , \tag{12}$$

where the function K_Q is defined by

$$K_Q\equiv\frac{T}{p}\frac{1}{1-e^{-E/T}}\ln\frac{\{x_2+\exp[-(E+\mu)/T)]\}[x_1+\exp(-\mu/T)]}{\{x_1+\exp[-(E+\mu)/T]\}[x_2+\exp(-\mu/T)]} \tag{13}$$

with

$$x_1=\exp\left[-\frac{E_{\max}}{T}\right]\ , \tag{14a}$$

$$x_2=\exp\left[-\frac{E_{\min}}{T}\right]\ , \tag{14b}$$

and

$$E_{\max}=\tfrac{1}{2}(E+p)\ , \tag{15a}$$

$$E_{\min}=\tfrac{1}{2}(E-p)\ . \tag{15b}$$

B. Rate in the hadronic phase

The production rate for dimuons in the hadronic (pion) phase is calculated along similar lines as in the quark-gluon phase. The main difference is that now resonance formation plays a prominent role. The diagram we consider for pion annihilation into leptons is shown in Fig. 5. In the Breit-Wigner approximation, where the form factor of the pion is given by a sum of ρ-like resonances,

$$F_\pi(M^2)=\sum_i\frac{g_{\rho_i\pi\pi}}{m_{\rho_i}{}^2-M^2-im_{\rho_i}\Gamma_{\rho_i}}\frac{m_{\rho_i}{}^2}{\gamma_{\rho_i}}\ . \tag{16}$$

In the vector-meson-dominance approximation only the ρ pole is kept in the summation and one has $g_{\rho\pi\pi}=\gamma_\rho$. The constants $g_{\rho\pi\pi}$ and γ_ρ can be obtained from the ρ decay into two pions and from the ρ decay into a lepton pair:

$$\Gamma(\rho\to\pi\pi)=(g_{\rho\pi\pi})^2\frac{m_\rho}{48\pi}\left[1-\frac{4m_\pi{}^2}{m_\rho{}^2}\right]^{3/2}\ , \tag{17a}$$

$$\Gamma(\rho\to e^+e^-)=\frac{4\pi\alpha^2}{3}\frac{m_\rho}{\gamma_\rho{}^2}\ . \tag{17b}$$

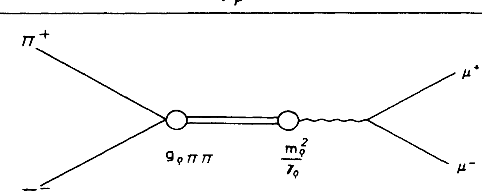

FIG. 5. Pion annihilation diagram.

This leads to the following approximate result for the pion form factor:

$$|F_\pi(M^2)|^2 \simeq \frac{(g_{\rho\pi\pi})^2}{\gamma_\rho^2}\left[\frac{m_\rho^4}{(m_\rho^2-M^2)^2+m_\rho^2\Gamma_\rho^2}+\left[\frac{g_{\rho'\pi\pi}}{g_{\rho\pi\pi}}\right]^2\frac{\gamma_\rho^2}{\gamma_{\rho'}^2}\frac{m_{\rho'}^4}{(m_{\rho'}^2-M^2)^2+m_{\rho'}^2\Gamma_{\rho'}^2}+\cdots\right] \tag{18}$$

or, in terms of decay widths, neglecting m_π vs m_ρ,

$$|F_\pi(M^2)|^2 \simeq \frac{(g_{\rho\pi\pi})^2}{\gamma_\rho^2}\left[\frac{m_\rho^4}{(m_\rho^2-M^2)^2+m_\rho^2\Gamma_\rho^2}+\frac{\Gamma(\rho'\to\pi\pi)}{\Gamma(\rho\to\pi\pi)}\frac{\Gamma(\rho'\to e^+e^-)}{\Gamma(\rho\to e^+e^-)}\frac{m_\rho^2}{m_{\rho'}^2}\frac{m_{\rho'}^4}{(m_{\rho'}^2-M^2)^2+m_{\rho'}^2\Gamma_{\rho'}^2}+\cdots\right], \tag{19}$$

where $\Gamma(\rho'\to e^+e^-)$ is known experimentally to be approximately equal to $\Gamma(\rho\to e^+e^-)$. Inserting the known values[9]

$$\Gamma(\rho'\to e^+e^-)\simeq 7.5\text{ keV}, \tag{20a}$$

$$\Gamma(\rho'\to\pi^+\pi^-)\simeq 60\text{ MeV}, \tag{20b}$$

$$\Gamma(\rho'\to\text{all})\simeq 260\text{ MeV}, \tag{20c}$$

leads to

$$|F_\pi(M^2)|^2 \simeq 1.2\frac{m_\rho^4}{(m_\rho^2-M^2)^2+m_\rho^2\Gamma_\rho^2}+0.12\frac{m_{\rho'}^4}{(m_{\rho'}^2-M^2)^2+m_{\rho'}^2\Gamma_{\rho'}^2} \tag{21}$$

which we will use subsequently as our model for the pion form factor.

At a first stage we present our results for the approximate expression derived from vector-meson dominance ($g_{\rho\pi\pi}=\gamma_\rho$),

$$|F_\pi(M^2)|^2 \simeq \frac{m_\rho^4}{(m_\rho^2-M^2)^2+m_\rho^2\Gamma_\rho^2}, \tag{22}$$

in order to allow more easy comparison with the numerical results of other calculations.

Proceeding as in the quark-antiquark annihilation case one obtains, for the production rate (use Bose-Einstein distributions for the pions),

$$\frac{dN_H}{d^4x\,d^4p}=\frac{\alpha^2}{48\pi^4}\left[1+2\frac{m_\pi^2}{M^2}\right]\left[1-4\frac{m_\pi^2}{M^2}\right]^{3/2}\times|F_\pi(M^2)|^2\exp\left[-\frac{E}{T}\right]K_H(p,T) \tag{23}$$

with the function $K_H(p,T)$ being defined as

$$K_H(p,T)\equiv\frac{T}{p}\frac{1}{1-\exp(-E/T)}\times\ln\frac{[x_2-\exp(-E/T)](x_1-1)}{[x_1-\exp(-E/T)](x_2-1)}. \tag{24}$$

The definitions of x_1 and x_2 remain unchanged but $E_{\max}$ and $E_{\min}$ are now given by

$$E_{\max}=\frac{1}{2}\left[E\left[1+\frac{m_\pi^2}{M^2}\right]+p\left[1-\frac{m_\pi^2}{M^2}\right]\right], \tag{25a}$$

$$E_{\min}=\frac{1}{2}\left[E\left[1+\frac{m_\pi^2}{M^2}\right]-p\left[1-\frac{m_\pi^2}{M^2}\right]\right]. \tag{25b}$$

Having thus established the basic formulas for the evaluation of the rate we now consider different mechanisms for the phase transition.

IV. DILEPTON RATE IN DIFFERENT SCENARIOS FOR THE PHASE TRANSITION

A. General remarks

The total dilepton rate is given by an integral over the space-time volume of the system. Because of the properties of Bjorken's scaling solution the appropriate variables are the proper time τ, the space-time rapidity y, and the transverse coordinates $x_\perp$ with $d^4x=\tau\,d\tau\,dy\,d^2x_\perp$. The thermodynamic quantities ϵ, p, s, and T only depend on τ and it is most appropriate to keep this as the final integration variable. In the scaling solution one identifies the space-time rapidity variable y with the fluid velocity rapidity θ. For the different scenarios we need four production rates.

(a) Dimuon production in the quark-gluon plasma phase with a cooling law given by

$$T=T_0\left[\frac{\tau_0}{\tau}\right]^{1/3}, \tag{26}$$

where T_0 is the initial temperature and τ_0 the proper time at which hydrodynamic expansions starts. This rate is given by

$$\frac{dN_Q(\text{hydro})}{dM^2d^2p_TdY}=\tfrac{1}{2}\int_{\tau_0}^{\tau_Q}\tau\,d\tau\int_{y_{\min}}^{y_{\max}}dy\,\frac{dN_Q}{d^4x\,d^4p}\times\left[T=T_0\left[\frac{\tau_0}{\tau}\right]^{1/3}\right], \tag{27}$$

where τ_Q is the proper time at which the system leaves the pure quark-gluon phase. The value of τ_Q differs considerably according to the considered mechanism. The rates are not strongly dependent on the limits of the space-time rapidity because the rapidity dependence is very much centered around the value of y (or θ)=0 as can be seen from Eq. (9). It is therefore a good approximation to cut off the rapidity integration at the value corresponding to the rapidity of the incoming beam.

(b) Dimuon production in the intermediate mixed phase from $q\bar{q}$ annihilation with the system still expanding but the temperature fixed at the critical temperature. This time the rate is given by

$$\frac{dN_Q(\text{mixed})}{dM^2 d^2p_T dY}=\frac{1}{2}\int_{\tau_Q}^{\tau_H}\tau\,d\tau\int_{y_{\min}}^{y_{\max}}dy\,f(\tau)\frac{dN_Q}{d^4x\,d^4p}\times(T=T_c)\ , \tag{28}$$

where τ_H is the proper time at which the system leaves the mixed intermediate phase. The function $f(\tau)$ is the fraction of the entropy in the quark-gluon phase:

$$s(\tau)=f(\tau)s_Q+[1-f(\tau)]s_H\ . \tag{29}$$

Since the temperature remains fixed at T_c, both s_Q and s_H remain constant but there is a continuous change from one phase to the other phase. It is very well known by now that the time spent in the intermediate phase is long because of the difference in the number of degrees of freedom:

$$\frac{\tau_H}{\tau_Q}=\frac{s_Q}{s_H}=\frac{37}{3} \tag{30}$$

so that τ_H is an order of magnitude larger than τ_Q. This stage is only present in the first-order equilibrium phase transition (Maxwell construction) and is completely absent in all other scenarios we consider. The function $f(\tau)$ is shown in Fig. 6.

(c) Dimuon production in the intermediate mixed phase from pion annihilation. The corresponding rate is given by

$$\frac{dN_H(\text{mixed})}{dM^2 d^2p_T dY}=\frac{1}{2}\int_{\tau_Q}^{\tau_H}\tau\,d\tau\int_{y_{\min}}^{y_{\max}}dy[1-f(\tau)]\frac{dN_H}{d^4x\,d^4p}\times(T=T_c)\ . \tag{31}$$

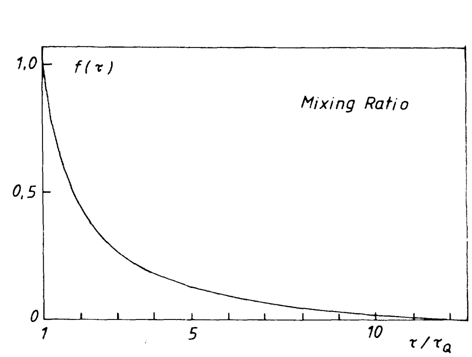

FIG. 6. Mixing ratio in the intermediate phase as a function of proper time; $f=1$ corresponds to pure quark-gluon phase.

(d) Dimuon production in the purely hadronic phase. The cooling law is given by

$$T=T_c\left[\frac{\tau_H}{\tau}\right]^{1/3}, \tag{32}$$

where T_c is the critical temperature and τ_H is the starting proper time of the hadronic phase. The rate is given by

$$\frac{dN_H(\text{hydro})}{d^4x\,d^4p}=\frac{1}{2}\int_{\tau_H}^{\tau_{f_0}}\tau\,d\tau\int_{y_{\min}}^{y_{\max}}dy\frac{dN_H}{d^4x\,d^4p}\times\left[T=T_c\left[\frac{\tau_H}{\tau}\right]^{1/3}\right], \tag{33}$$

where τ_{f_0} is the value of the eigentime at which the system reaches the freeze-out temperature.

B. First-order phase transition (equilibrium)

For a first-order phase transition at equilibrium the temperature evolution with proper time is as shown in Fig. 1. The rate for dilepton production is obtained by adding the four contributions given above [(a),(b),(c), and (d)]. The simple vector-dominance model for the pion form factor gives the rate shown in Fig. 7. Below $M=1$ GeV the hadronic contribution dominates while above $M=2.5$ GeV the quark-phase contribution dominates. Intuitively this can be understood easily: to produce high-mass lepton pairs one needs high temperatures and these are only available in the initial quark phase, correspondingly the colder hadronic phase produces many low-mass lepton pairs. There is a region of width 1 GeV where both phases are prominently present. This reflects the presence of the intermediate region where both phases coexist at the same temperature and thus contribute similarly to the production rate. The production mechanism changes smoothly from quark-antiquark annihilation to

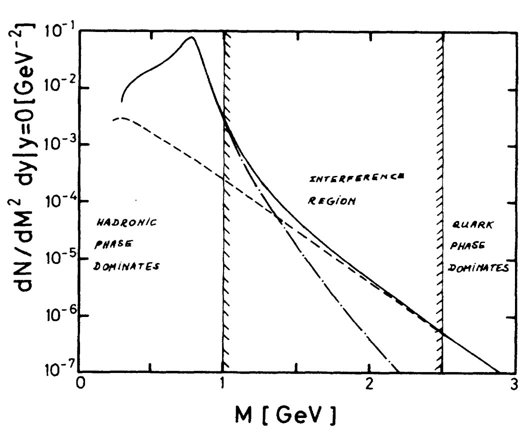

FIG. 7. Cross section for the production of muon pairs calculated for the equilibrium first-order phase transition. Dashed-dotted line—hadron contribution; dashed line—quark contribution; solid line—sum of quark and hadron contributions; T_0 is taken to be $T_0=284$ MeV, $\tau_0=1$ fm, $T_c=227$ MeV, $T_{f_0}=154$ MeV.

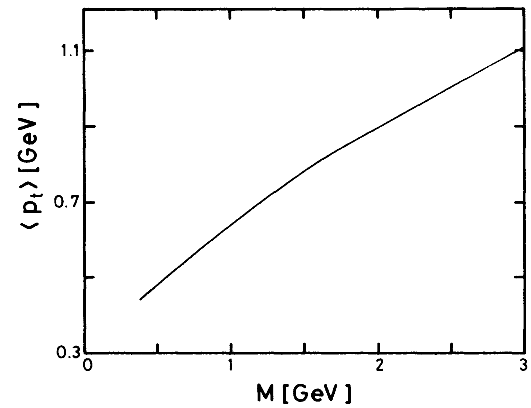

FIG. 8. Average transverse momentum $\langle p_t \rangle$ of the lepton pairs. The phase transition is equilibrium first order and parameters as in Fig. 7.

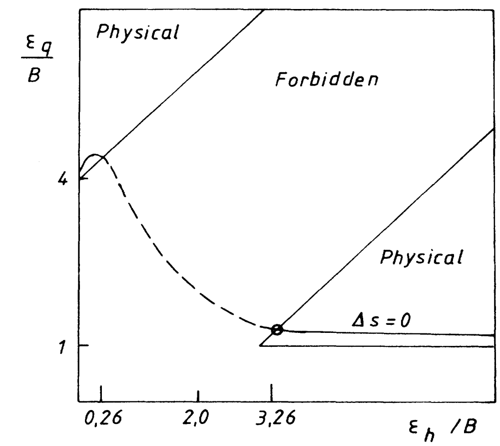

FIG. 10. Allowed and forbidden region s in the ϵ_q,ϵ_h plane.

pion annihilation. The average transverse momentum $\langle p_T \rangle$ follows this trend and the derivative of $\langle p_T \rangle$ as a function of M indicates no structure as one sweeps over the M range. This is shown quantitatively in Figs. 8 and 9.

C. Supercooling with subsequent superheating

If the rate of hadronization is not fast enough compared to the expansion rate, a substantial amount of supercooling will occur. It is not known at present how much supercooling is likely to occur and we concentrate our attention on mechanisms where supercooling is as little as possible. To calculate the amount of supercooling we work with a model where a sharp front exists separating the hadronic from the quark-gluon-plasma phase. Energy and momentum conservation in the form of conservation of the energy-momentum tensor

$$\partial_\mu T^{\mu\nu}=0 \tag{34}$$

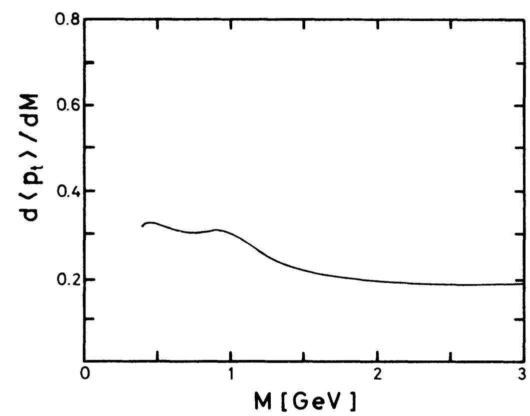

FIG. 9. Derivative of the average transverse momentum with respect to the invariant mass of the lepton pair for first-order equilibrium phase transition. Parameters as in Fig. 7.

relates the temperatures, pressures, and energy densities existing on each side of the front. This analysis has been carried out in Ref. 1. The most stringent constraint comes from the entropy law leading to an increase of entropy across the front:

$$\partial_\mu s^\mu \geq 0 \ , \tag{35}$$

where $s^\mu \equiv s u^\mu$.

The energetically allowed transition region is shown in the ϵ_q,ϵ_h plane in Fig. 10. We indicate by a small circle the region with the smallest amount of superheating and indicate in Fig. 2 the resulting jump in temperature.

The corresponding dilepton spectrum is given by a sum of two terms [(a) and (d) above]:

$$\frac{dN(\text{detonation})}{dM^2dY\,d^2p_T}=\frac{dN_Q(\text{hydro})}{dM^2dY\,d^2p_T}+\frac{dN_H(\text{hydro})}{dM^2dY\,d^2p_T} \ . \tag{36}$$

We assume that the violent jump from one phase to the other is approximately instantaneous and therefore contributes very little to the dilepton production rate. The results from Eq. (36) are shown in Fig. 11. This time there is no region in M where the quark-gluon-plasma phase dominates. Intuitively this can be understood as follows: after the detonation takes place, the resulting hadronic phase is very much superheated and dileptons can be produced in a broad mass range. There is a smooth evolution in the average transverse momentum as a function of the invariant mass (Fig. 12). A different mechanism was considered recently in Ref. 10. This can be obtained from the detonation mechanism described above if the velocities on both sides of the front are the same. With a sharp front this is inconsistent with the constraints of energy and momentum conservation. At best it might be conceivable if their mechanism is viewed as a bulk volume transition where no sharp front exists. In their considerations the energy density remains the same: thus, $\epsilon_q(T_q)=\epsilon_h(T_h)$. This leads also to a discontinuity in the temperature but a much weaker one. Since this mechanism is not consistent with the hydrodynamic equations of motion we do not consider it further.

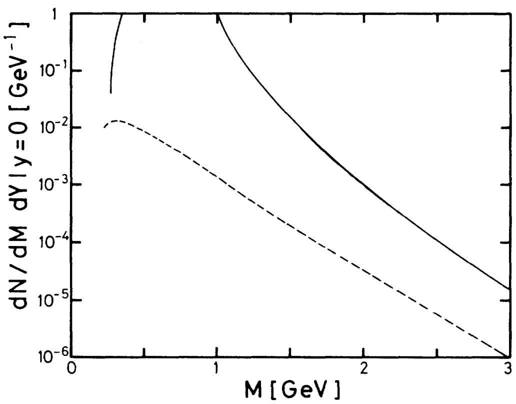

FIG. 11. Cross section for the production of muon pairs in first-order detonation phase transition. Dashed line—pure quark contribution; solid line—hadron plus quark contribution. Parameters as in Fig. 7.

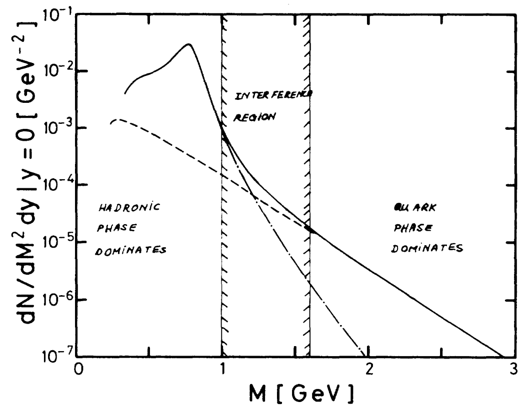

FIG. 13. As in Fig. 7 but for second-order phase transition.

D. Second-order phase transition

With a second-order phase transition the system changes its phase instantaneously at a critical eigentime τ_c upon reaching the critical temperature. A first estimate of the rate for dilepton production is obtained by summing contributions (a) and (d) above:

$$\frac{dN(\text{second order})}{dM^2dY\,d^2p_T}=\frac{dN_Q(\text{hydro})}{dM^2dY\,d^2p_T}+\frac{dN_H(\text{hydro})}{dM^2dY\,d^2p_T}\ . \tag{37}$$

The result is shown in Fig. 13 for the vector-meson-dominance form of the pion form factor.

In Fig. 13 one observes that the quark-gluon phase dominates for large values of the invariant mass M and the hadronic phase dominates for small values. There is, however, one striking feature: from Figs. 7 and 13 one notices that the region where both phases have comparable contributions is considerably smaller for a second-order phase transition. In other words, there is now a cleaner separation between the region dominated by the hadronic phase and the region dominated by the quark-gluon-plasma phase. The origin of this can be traced back to the fact that there is a clean break in proper time between the two phases. Also the temperature is always consistently higher in the quark-gluon phase than in the hadronic phase. This is reflected in the average transverse momentum of the dilepton pair shown in Fig. 14 which shows a relatively clean break around $M=1$ GeV corresponding to the tail of the contribution from the ρ resonance. To enhance this feature we show the derivative of $\langle p_T \rangle$ with respect to M in Fig. 15.

To investigate this interesting feature in more detail we consider a series of modifications to the above treatment which we discuss in the following.

1. Variations on temperature

Bearing in mind the possible errors typical for the lattice Monte Carlo calculations and also those connected with the hopping-parameter expansion we have considered

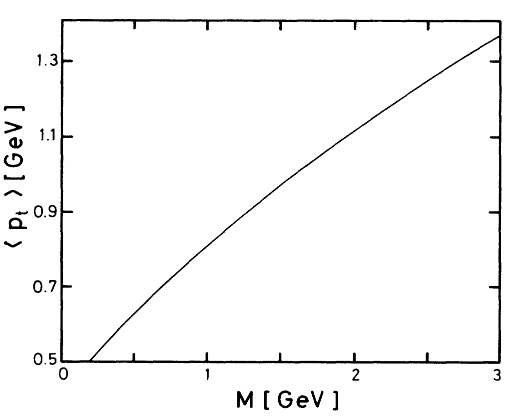

FIG. 12. Average transverse momentum vs invariant mass for a detonation with parameters as in Fig. 7.

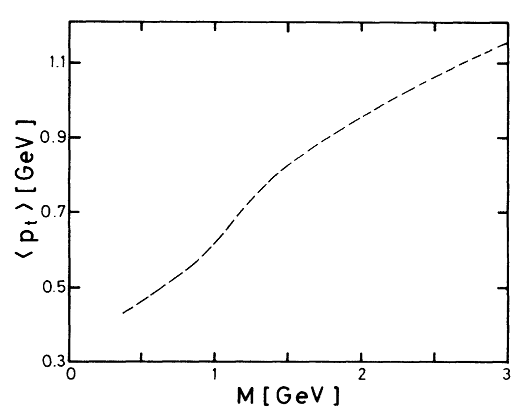

FIG. 14. $\langle p_t \rangle$ vs invariant mass for second-order phase transition and parameters as in Fig. 7.

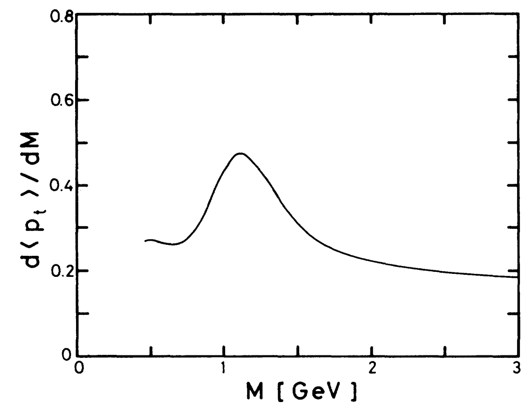

FIG. 15. Derivative of the $\langle p_t \rangle$ distribution with respect to invariant mass M for second-order phase transition with the parameters as in Fig. 7.

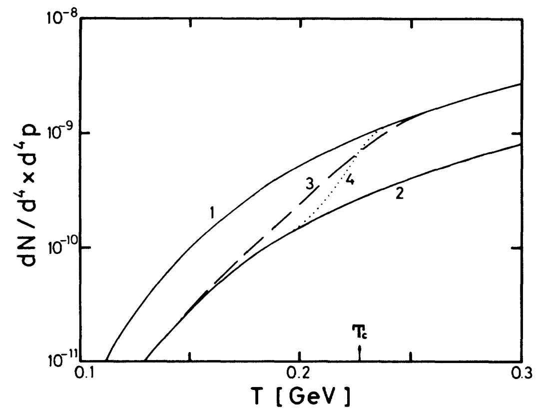

FIG. 16. Interpolation in temperature between pure-quark (curve 1) and pure-hadron (curve 2) rate. Dotted curve corresponds to $n=30$; dashed curve corresponds to $n=10$.

variations in the functional dependence of the temperature on eigentime. We have observed that even if the temperature $T(\tau)$ is very close to the first-order Maxwell transition curve (Fig. 1), the bump structure still persists. This is because the contribution of the mixed phase to the production rate is in general different from the contributions arising from the corresponding quark-gluon and hadronic phases in the same interval of eigentime for the second-order phase transition.

2. *Influence of smoothing*

In terms of the considered model[2] the electromagnetic current-current correlation function related to the production rate of dimuons is discontinuous across a phase transition. When the second-order phase transition is assumed in the system, the current correlation function $\langle J^{\mu}(x)J^{\nu}(0)\rangle$ should presumably be a continuous function in the full region of temperature. This is due to the long-range correlations in the transition region for a second-order phase transition. It could happen that the observed jump in the $d\langle p_T \rangle /dM$ distribution is due to the above singular behavior of the model at $T=T_c$.

In order to examine this possibility we performed an interpolation between the thermal rate formulas valid below and above critical temperature (Fig. 16). The contribution of the quark-gluon phase was multiplied by a factor

$$1-\exp\left[-\left[\frac{T}{T_c}\right]^n\right]$$

with n being a large number (typically between 10 and 30). Correspondingly, the contribution of the hadronic phase was multiplied by the complement of the above factor, namely,

$$\exp\left[-\left[\frac{T}{T_c}\right]^n\right].$$

In this way the transition is spread out over a range of temperature values corresponding approximately to the spread observed in results from lattice QCD. The resulting lepton rate is, however, not modified appreciably. We have also considered a spreading in terms of the energy density instead of the temperature but again the signal in $d\langle p_T \rangle /dM$ survived the smoothing transition. This is shown in Fig. 17.

3. *Influence of other resonances*

As the change in transverse momentum occurs at the tail of the ρ resonance we investigated also the influence of the higher resonances, in particular the $\rho'(1600)$. The results obtained here show that there is a clear connection between the observed behavior and the presence of resonances. The interference pattern we obtain this way is shown in Figs. 18—20.

4. *First-order equilibrium phase transition with very high initial temperature*

Since the ρ' contribution occurs in the region where considerable overlap occurs between the two phases in the first-order phase transition scenario we have also investi-

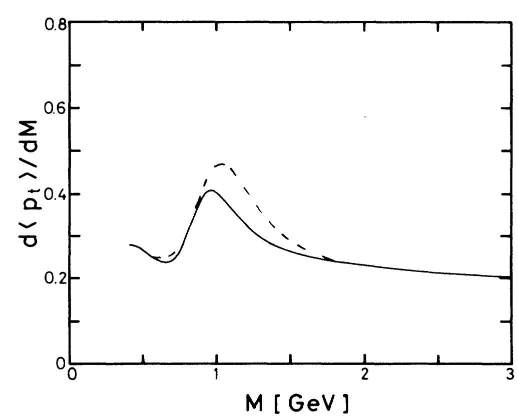

FIG. 17. As in Fig. 15 but computed with interpolated rate formula. $n=10$—solid curve; $n=30$—dashed curve.

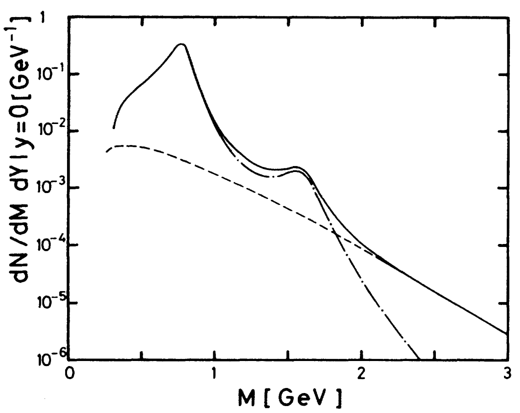

FIG. 18. As in Fig. 13 but with $\rho'(1600)$ resonance taken into account.

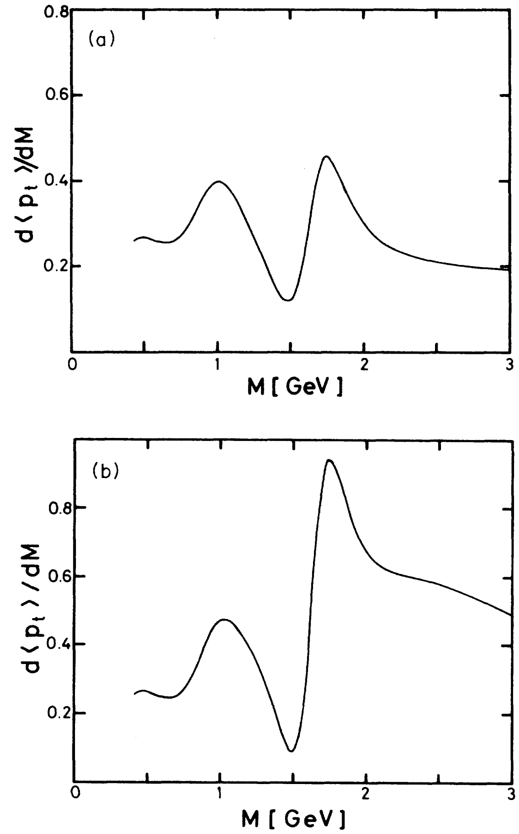

FIG. 20. Derivative of $\langle p_t \rangle$ vs invariant mass M with $\rho'(1600)$ resonance taken into account for second-order phase transition (a) with initial temperature $T_0 = 284$ MeV, (b) with $T_0 = 1.1$ GeV.

gated the influence of a very high initial temperature in this case. By changing the initial temperature one increases the contribution from the quark-gluon phase to the dilepton production rate. It is thereby possible to tune this contribution such that it will start dominating immediately after the tail of the ρ' peak (Fig. 21). This occurs for an initial temperature of the order of 1 GeV and produces a pronounced change in the average transverse momentum shown in Fig. 22. It is, however, of interest to note that in this case the structure in the tail of the ρ meson is not very pronounced.

V. SUMMARY AND CONCLUSIONS

In this work we investigated the dilepton yield in ultrarelativistic nuclear collisions in different scenarios for the phase transition from quarks and gluons to hadrons. The relevant kinematical variables are the invariant mass M and the transverse momentum p_T of the lepton pair. High values of the invariant mass M can only be reached if the temperature of the system is high while correspondingly low values of M rise mainly from the system being at low temperatures. Therefore, M is the relevant variable to distinguish between the quark-gluon plasma contribution and the hadronic phase contribution. We then focused our attention on the intermediate region where the system changes from one phase to the other and thus interesting information about the phase transition scenario can be expected. The invariant mass can, roughly speak-

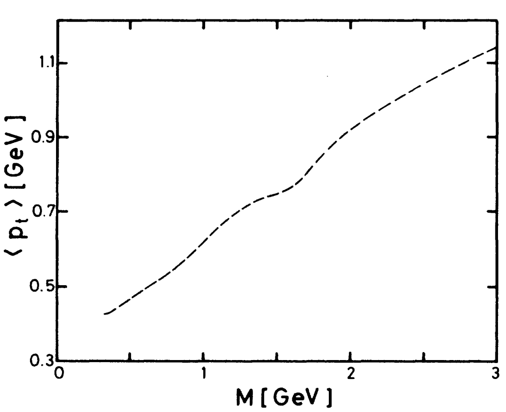

FIG. 19. As in Fig. 14 but with $\rho'(1600)$ resonance taken into account.

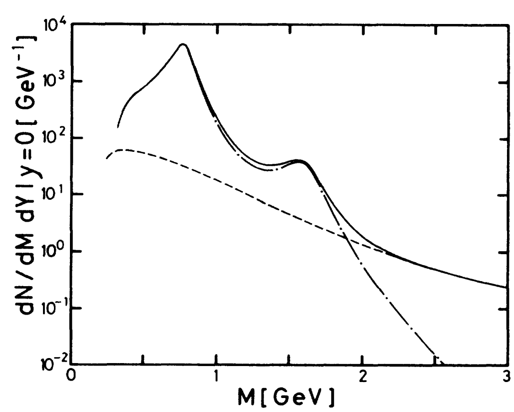

FIG. 21. As in Fig. 7 but including contribution from $\rho'(1600)$ resonance.

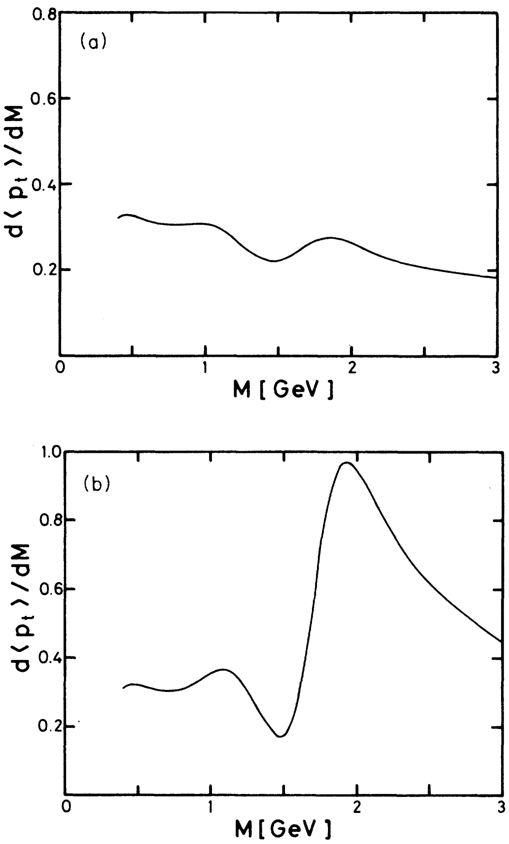

FIG. 22. Derivative of $\langle p_t \rangle$ vs invariant mass with $\rho'(1600)$ taken into account for first-order equilibrium phase transition (a) $T_0 = 284$ MeV, (b) $T_0 = 1.1$ GeV.

ing, be considered as representing either the temperature of the system or the eigentime. High invariant masses correspond to early times or high temperatures while low invariant masses correspond to late times or low temperatures. The region in between can tell us something about the nature of the transition. In the first scenario we investigated, namely, a first-order phase transition with the system always being in thermal equilibrium, there exists a long-lived intermediate region where both phases coexist at the same critical temperature. In this case we found a smooth transition from one region to the other and no abrupt changes in the transverse momentum. In the second scenario the quark-gluon plasma phase undergoes substantial supercooling before making a transition to superheated hadronic matter via a detonation. Here we found that the hadronic phase dominates the dilepton production rate over the whole invariant-mass range considered. No information can thus be obtained on the quark-gluon plasma phase in this scenario. A second-order phase transition is characterized by an instantaneous transition from one phase to the other. This leads to a clean separation between each phase in the invariant mass M. Consequently, there is a noticeable change in the transverse-momentum variable when M is between 1 and 1.5 GeV. To enhance this change we considered the derivative $d\langle p_T \rangle /dM$ as a function of M. A clear jump is seen here when crossing the intermediate region. This is due to the interference between the quark-gluon phase and hadronic phase contributions to the dilepton yield. It is interesting to note that the observed jump appears for realistic values of the parameters (initial temperature = 284 MeV, freeze-out temperature = 154 MeV) and is enhanced when increasing the initial temperature.

To investigate this interesting feature further we considered a series of modifications to the scenarios discussed above. We performed an interpolation, in temperature as well as in energy density, between the thermal rates below and above the critical temperature T_c. The bump in $d\langle p_T \rangle /dM$ decreases but does not disappear completely. Even in the case when the interpolation is performed in quite a large-temperature interval (0.15—0.24 GeV) the bump in $d\langle p_T \rangle /dM$ decreases only by about 20%. The structure of the $\langle p_T \rangle$ distribution similar to the one obtained in the second-order phase transition can also be found with other scenarios if one increases substantially the initial temperature. It is the outstanding property of a second-order phase transition that the bump already appears for low values of the initial temperature. We conclude therefore that the region between 1 and 2 GeV in invariant mass for the lepton pair is sensitive to the dynamical mechanism for the phase transition from quarks and gluons to hadrons.

Finally, let us consider the dependence of our results on the assumptions made to derive them. First of all, we will consider the influence of the equation of state on the behavior of p_T as a function of the invariant mass M. For the case of a first-order phase transition we have used the bag-model equation of states above T_c and ideal-gas equation of state below T_c. This assumption has been frequently used in the literature.[2] It is presumably far away from reality, especially around T_c. The numerical analysis of lattice QCD does suggest that just above T_c gluons behave as an ideal gas; however, the inclusion of quarks leads to a behavior which is far away from the ideal-gas type. This can be seen in Fig. 3 and also from recent Monte Carlo data.[11] The importance of interactions just above T_c has been discussed recently by DeGrand.[12] Also in the hadronic pion gas phase interactions can lead to significant deviations from the ideal-gas equation of state. Thus one can easily imagine a situation where the system undergoes a first-order phase transition but due to interactions the latent heat is much smaller than in the case we have considered. In such a case the contribution from the mixed phase to the dilepton production will be small and the overlap region between pure quark-gluon phase and pure hadronic phase contributions will decrease significantly. As a consequence the nontrivial structure in the p_T vs M distribution could be presumably observed already for reasonably small values of the initial temperature. Otherwise, such a structure appears only for initial temperatures of the order of 1 GeV [see Fig. 22(b)]. Our results suggest that the most significant change in dp_T/dM is obtained in the limit where the production of latent heat goes to zero, which is the limit where the first-order phase transition becomes a second-order one. For the case of a second-order phase transition we have used the equation of state from lattice QCD results which we consider to be the realistic equation of state. The purpose of our analysis was to indicate the influence of the equations of state on the p_T behavior taking as a basis the equation of state for a strong first-order phase transition (as given by the bag model) and comparing it to a second-order phase transition with equation of state taken from lattice gauge theory.

The second assumption in our considerations concerns the formulas for thermal rates used in the computations. For the strong first-order phase transition the rates have been computed following suggestions made previously in the literature.[2] In general, however, the behavior of the electromagnetic current-current correlation function in strongly interacting matter cannot be computed at present in terms of one model which admits a phase transition. Such a computation could be performed using lattice QCD but the lattice size presently available is too small for this kind of analysis. In this point our results strongly depend on the assumption we have made for the thermal rates formulas. For the second-order phase transition case we have used modifications of the thermal rates formulas in order to assure continuity across the phase transition. All results presented in Figs. 16—22 dealing with a second-order phase transition have been obtained using the modified formula for rates. As we indicate this modification does not significantly change the results obtained using the lattice QCD equation of state. Thus in terms of the model considered we can clearly see the difference between a strong first-order and a second-order phase transition. However, for a weak first-order phase transition, because of uncertainties in the behavior of the thermal rates we are not able on the level of our approach to see a difference with a second-order phase transition because the equations of state for both of these transitions will be very similar and also the rates have similar behavior across the phase transition.

There is, however, an interesting feature of the analysis which seems to be common to equilibrium first- and second-order phase transitions. This is the general structure of p_T as a function of the invariant mass. If there is no quark-gluon-plasma formation, then the p_T distribution is a smooth function of M and does not show any structure even for very high initial temperatures (see Fig. 23). If there is, however, a first- or second-order phase transition in the system then a nontrivial structure (Figs. 16—22) can be observed. The only difference we have

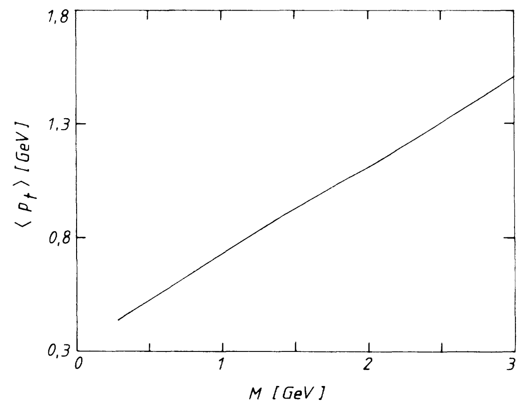

FIG. 23. $\langle p_t \rangle$ vs invariant mass for pure hadron gas with $T_0 = 1.1$ GeV and other parameters as in Fig. 7.

seen between strong first- and second-order phase transitions is that for the former this structure is seen only for very large initial temperatures. The observed behavior of p_T on M seems to be connected with the resonance structure of the hadronic dilepton production process and appears due only to the interference between pure hadronic and pure quark contributions just above the position of the resonance. Thus our results suggest that observation of a structure as shown in Figs. 16—22 would be evidence for the production of a quark-gluon plasma. One could also imagine a scenario where the first-order phase transition proceeds via a detonation wave. In this case the hadronic phase completely dominates the dilepton production rate; therefore, naturally, one will not observe any structure in the p_T distribution. Thus the behavior shown in Figs. 16—22 is not a necessary but rather a sufficient condition to conclude that a quark-gluon plasma was produced.

ACKNOWLEDGMENTS

We acknowledge very useful discussions with Larry McLerran, Helmut Satz, Rudolf Baier, E. Hilf, and G. Franke. One of the authors (J.C.) acknowledges financial support from the Council of Scientific and Industrial Research, Faure, South Africa. Another (K.R.) acknowledges the financial support of the Alexander von Humbolt Foundation.

*Permanent address: Institute of Theoretical Physics and Astrophysics, University of Cape Town, 7700 Rondebosch, Republic of South Africa.

†On leave of absence from the Institute for Theoretical Physics, University of Wrocław, Wrocław, Poland.

[1]M. Gyulassy, K. Kajantie, H. Kurki-Suonio, and L. D. McLerran, Nucl. Phys. **B237**, 477 (1984).

[2]E. L. Feinberg, Nuovo Cimento **34A**, 391 (1976); E. V. Shuryak, Phys. Lett. **78B**, 150 (1978); G. Domokos and J. I. Goldman, Phys. Rev. D 23, 203 (1981); G. Domokos, *ibid.* **28**, 123 (1983); S. Chin, Phys. Lett. **119B**, 51 (1982); L. D. McLerran and T. Toimela, Phys. Rev. D 31, 545 (1985); R. C. Hwa and K. Kajantie, *ibid.* **32**, 1109 (1985); K. Kajantie, J. Kapusta, L. McLerran, and A. Mekjian, *ibid.* **34**, 2746 (1986);

J. Cleymans and J. Fingberg, Phys. Lett. **168B**, 405 (1986).
[3]J. D. Bjorken, Phys. Rev. D **27**, 140 (1983).
[4]J. Cleymans, R. V. Gavai, and E. Suhonen, Phys. Rep. **130**, 217 (1986).
[5]L. van Hove, Z. Phys. C **21**, 93 (1983); **27**, 135 (1985).
[6]K. Redlich and H. Satz, Phys. Rev. D **33**, 3747 (1986).
[7]T. Celik, J. Engels, and H. Satz, Nucl. Phys. **B256**, 670 (1985).
[8]Our notation follows McLerran and Toimela (Ref. 2).
[9]Particle Data Group, Phys. Lett. **107B**, 1 (1986).
[10]J. Kapusta and A. Mekjian, Phys. Rev. D **33**, 1304 (1986).
[11]*Lattice Gauge Theory, 1986,* edited by H. Satz *et al.* (Plenum, New York, in press).
[12]T. A. DeGrand and C. E. DeTar, in *Lattice Gauge Theory, 1986* (Ref. 11).